Noise-Temperature Measurement System for the WR-28 Band

J. Randa
L.A. Terrell

Electromagnetic Fields Division
Electronics and Electrical Engineering Laboratory
National Institute of Standards and Technology
325 Broadway
Boulder, Colorado 80303-3328

CONTENTS

NOISE-TEMPERATURE MEASUREMENT SYSTEM
FOR THE WR-28 BAND

J. Randa and L. A. Terrell

Electromagnetic Fields Division

National Institute of Standards and Technology

Boulder, CO 80303

The NIST Noise Project has constructed and tested a radiometer for the measurement of noise sources in the WR-28 waveguide band (26.5 GHz to 40 GHz). It is a total-power radiometer which incorporates a six-port reflectometer for the measurement of relevant reflection coefficients. The radiometer is similar in design to existing NIST systems covering the WR-62 (12.4 GHz to 18 GHz) and WR-42 (18 GHz to 26.5 GHz) bands. This paper reviews the theory and describes the design, testing, and operation of the system. Because of the similarities between the present system and the existing WR-62 and WR-42 systems, much of this document also applies to those systems.

Keywords: noise; noise measurement; noise temperature; radiometer; thermal noise

1. BACKGROUND

1.1 Introduction

The NIST Noise Project has recently completed the construction and testing of a system for the measurement of the noise temperatures of sources with WR-28 output flanges. The system covers the entire frequency range of the WR-28 band, 26.5 GHz to 40.0 GHz. It extends NIST waveguide noise capabilities, which already comprise systems for the WR-90 (8.2 GHz to 12.4 GHz), WR-62 (12.4 GHz to 18 GHz), and WR-42 (18 GHz to 26.5 GHz) frequency bands. The WR-90 system uses a switching scheme originally proposed by Dicke [1]. Its design and operation are described in reference [2]. The WR-62 and WR-42 systems are total-power radiometers which incorporate six-port reflectometers to measure relevant reflection coefficients. The general design and underlying theory for these systems and similar coaxial systems are covered in reference [3]. Details of the design of the waveguide systems, the tests used in the initial checkout of the systems, and actual measurement procedures have not been published for the waveguide systems.

This paper reports the design, system checks, and operational procedures of the new WR-28 system. Since descriptions and details of the other similar NIST systems have not been published, the present account will also serve as a description of their design, checkout, and operation. The remainder of the paper is organized as follows. The next subsection reviews the theory underlying noise-temperature measurements with a total-power radiometer and derives the radiometer equation. Section 2 gives a detailed description of the measurement system. In Section 3 we review the steps used to make a noise-temperature measurement with the system. Section 4 presents the checkout procedure, including a review of the different tests which ensure that the system is functioning properly. The uncertainty analysis for the WR-28 system is presented in Section 5, and the paper closes with a brief summary in Section 6.

2

1.2 Radiometer Equation

Conceptually, derivation of the radiometer equation for the total-power radiometer is quite simple. The radiometer is assumed to respond linearly to the power delivered to it. Generally, the linear response varies as a function of the impedance of the source, but our radiometers for 1 GHz and above all have sufficient input isolation that their response can be taken to be independent of the impedance of the source. The radiometer therefore requires two known delivered powers for its calibration. The standards used are noise-temperature standards, which have a known *available* power rather than delivered power. We must correct for loss and mismatch to relate the delivered powers to the known available powers. Once the radiometer is calibrated, it is used to measure the delivered power from the device under test (DUT). We then correct for mismatch and loss in the DUT measurement to obtain its available power and consequently its noise temperature.

Before proceeding, we establish some notation and conventions. We use the term noise temperature to mean the spectral density of available power from the source, divided by Boltzmann's constant. Thus for a small bandwidth B, over which the available power density is constant, the available power is given by $P = k_B B T_n$. Available powers will be denoted by capital P, and delivered powers by lowercase p. The subscript on an available power generally indicates the device, except in the case of P_a, where it indicates the ambient, $P_a = k_B B T_a$. The subscript a will denote ambient, s will denote the cryogenic standard, and x will denote the DUT.

To derive the explicit expression for the radiometer equation, we refer to the simplified block diagram of figure 1. The subscripts on the delivered powers and mismatch factors will indicate the reference plane and the configuration. Thus p_{0x} refers to the delivered power at plane 0 when the DUT (x) is connected. For an isolated radiometer, the derivation follows the basic treatment by Daywitt [3], with a few notational changes. When the switch is connected to the DUT at plane 2, the noise temperature at plane 0 is related to the DUT noise temperature T_x by
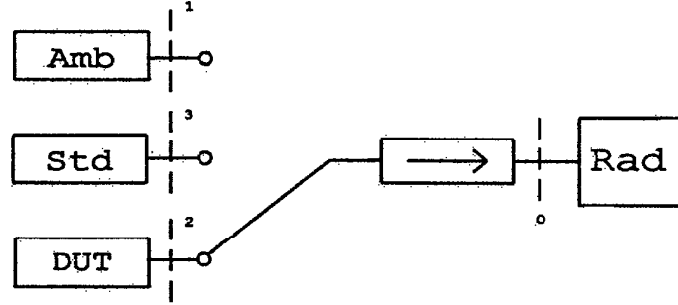
Figure 1. Basic setup for measurement of noise temperature.

$$P_{0,x} = \alpha_{02} P_x + [1 - \alpha_{02}] P_s , \qquad (1)$$

where $\alpha_{02} = P_0/P_2$ is the available-power ratio between planes 2 and 0. The delivered power is then given by

$$p_{0,x} = M_{0,x} \alpha_{02} P_x + M_{0,x} [1 - \alpha_{02}] P_s + p_{ex} , \qquad (2)$$

where p_{ex} is the intrinsic effective input noise power of the radiometer for this configuration, and $M_{0,x}$ is the mismatch factor at plane 0 when the switch is connected to the DUT x. Similarly,

$$p_{0,s} = M_{0,s} \alpha_{03} P_s + M_{0,s} [1 - \alpha_{03}] P_s + p_{es} ,$$

$$p_{0,a} = M_{0,a} P_a + p_{ea} . \qquad (3)$$

Due to the isolator to the left of plane 0, the intrinsic effective input noise power of the radiometer is (approximately) independent of the source configuration, $p_{ex} \approx p_{es} \approx p_{ea}$. Combining eqs (2) and (3), and using the relation $P = k_B B T$, we obtain

$$T_x = T_a + (T_s - T_a) \frac{M_{0,s} \alpha_{03}}{M_{0,x} \alpha_{02}} \frac{Y_x - 1}{Y_s - 1} + (\Delta T_x)_{is} , \qquad (4)$$

where $Y_x = p_x/p_a$, $Y_s = p_s/p_a$, and $(\Delta T_x)_{is}$ is the error in T_x due to the (small) effect of an imperfect isolator. Equation (4) can be put in Daywitt's form by noting that $M_{0,s} \alpha_{03} = M_3 \eta_{03}$ and $M_{0,x} \alpha_{02} = M_2 \eta_{02}$, where the efficiency η_{ij} is defined as the ratio of the delivered powers at

4

planes i and j, $\eta_{ij} \equiv p_i/p_j$. In addition, we neglect $(\Delta T_x)_{ij}$ and include its effect in the uncertainty. The radiometer equation then assumes the form

$$T_x = T_a + (T_\beta - T_a) \frac{M_3 \eta_{03}}{M_2 \eta_{02}} \frac{Y_x - 1}{Y_\beta - 1} \; . \tag{5}$$

Equation (5) is the form of the radiometer equation which is used in measurements of noise temperature on the NIST waveguide systems. The noise temperatures appearing on the right side of the equation are those of the ambient and cryogenic standards and are therefore known. The Y's are the ratios of measured powers. The mismatch factors M_2 and M_3 are determined from

$$M_2 = \frac{(1 - |\Gamma_x|^2)(1 - |\Gamma_{2,R}|^2)}{|1 - \Gamma_x \Gamma_{2,R}|^2} \; ,$$

$$M_3 = \frac{(1 - |\Gamma_\beta|^2)(1 - |\Gamma_{3,R}|^2)}{|1 - \Gamma_\beta \Gamma_{3,R}|^2} \; , \tag{6}$$

where the reflection coefficients are measured with the six-port reflectometer built into the system, and the subscript R indicates that the reflection coefficient is from the radiometer at the plane indicated. We refer to the ratio of efficiencies, η_{03}/η_{02}, as the asymmetry; it is evaluated by the method described in reference [3] and Section 3 below.

2. SYSTEM DESCRIPTION

The radiometer system is similar in design to other NIST radiometers with internal six-port reflectometers [3]. Diagrams of the system, showing different degrees of detail, are given in figures 2(a) and 2(b). Figure 2(a) presents a somewhat simplified diagram, in which it is easier to follow the measurement flow and to distinguish between the six-port and the noise-power subsystems. Figure 2(b) shows a more complete schematic, with various components labelled to facilitate discussion. In both figures, the switches are set for a six-port measurement. The switch S3 between the low-pass filter LPF1 and the mixer is switched to the down position to make the noise-power measurements. Similarly, switch S2 switches the local oscillator (LO) to the mixer and away from the six port for noise-power measurements.

5
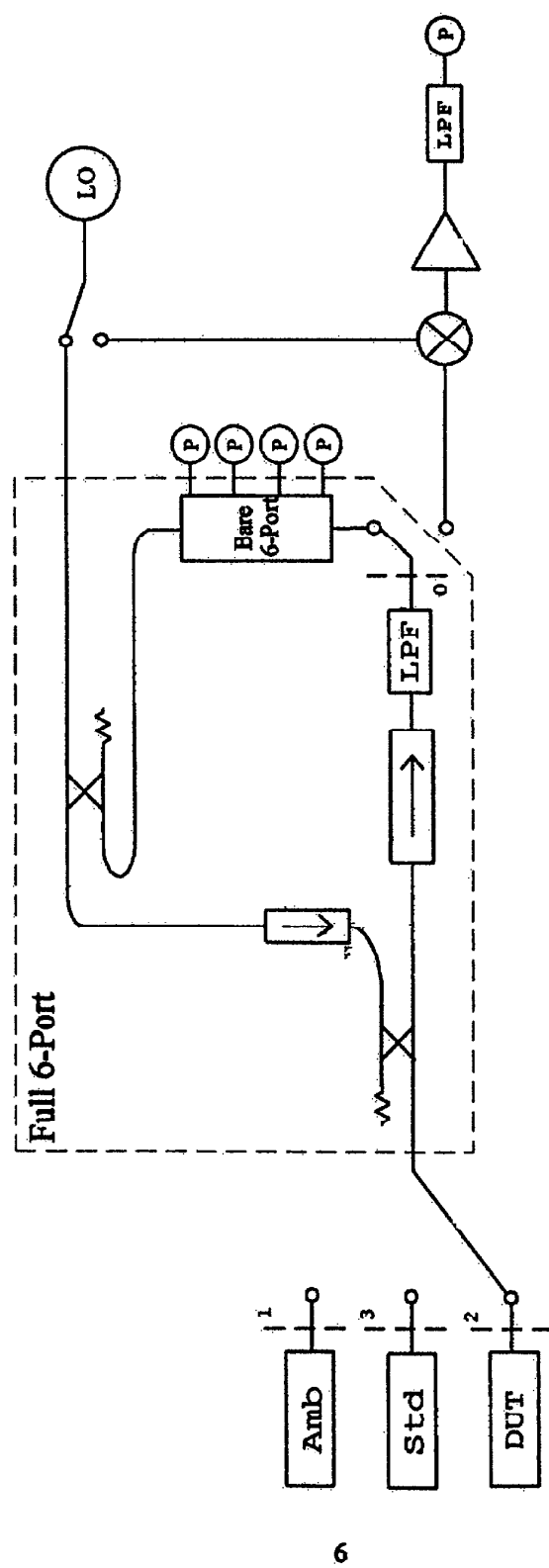
Figure 2(a). Simplified diagram of radiometer, with switches set for six-port measurement.

6

Figure 2(b). Schematic of WR-28 radiometer.

7

A manual switch (S1) is used on the front end to select among the three sources, the ambient standard, the cryogenic standard, and the DUT. The noise measurement path proceeds through two 27 dB isolators (I1 and I2) and a filter, to the mixer. The frequency of the local oscillator signal to the mixer is set to the nominal measurement frequency. The down converted signal from the mixer is amplified and then filtered to pass only frequencies below 20 MHz. The power emerging from the filter is measured by a NIST type-IV power meter [4]. The combined gain of the intermediate-frequency (IF) amplifiers is about 57 dB. The power measured by the power meter is typically a few milliwatts. The noise power spectral density available from the noise source ranges from about 1 fW/MHz for the cryogenic standard to about 0.14 pW/MHz for a typical "hot" (10 000 K) source.

The six-port reflectometer built into the system is used to measure reflection coefficients of the sources and of the ports at which the sources are connected. These reflection coefficients are used to compute the mismatch factors at planes 2 and 3. The six-port is calibrated by attaching a series of impedance standards (flat short, sliding short, sliding load) to the port of interest [5,6]. The source used as the local oscillator is a Gunn diode for the WR-28 system. Three different diodes are used to span the WR-28 band. For the WR-62 and WR-42 systems a frequency synthesizer is used, but power and financial considerations dictated use of the Gunn diode source for WR-28. The coupler and sensor in the LO arm are used to measure the frequency in locking the diode. The variable attenuator A1 is used to set the LO power to a convenient level for the six-port measurements and for the noise power measurements. The low-pass filter (LPF1) for the WR-28 system has a cutoff frequency of about 45 GHz. It prevents harmonics of the measurement frequency from reaching the mixer. The preamplifier immediately following the mixer is not present in the WR-62 and WR-42 systems. The IF box of figure 2(b) is housed in an electronics rack and is used with all the waveguide systems. The input switch configuration of the IF box allows several systems to be connected simultaneously. The variable attenuators A3 and A4 are used to check the linearity of the IF unit, and the low-pass filter LPF2 cuts off at 20 MHz. The switch (S4) in front of the power meter P5 allows periodic dc bias readings for the meter.

8

Two noise-temperature standards are used to calibrate the system for each measurement of a DUT. One is a cryogenic standard, described in detail in references [7] and [8]. It consists of a specially designed horn antenna, looking into a cavity containing silicon carbide pyramids immersed in liquid nitrogen. The silicon carbide pyramids constitute a blackbody radiator at a known physical temperature, the boiling temperature of liquid nitrogen. The thermal radiation characteristics of such a surface are known and can be used to calculate the available power at the output reference plane [8], which is taken to be at the flange of the WR-28 waveguide emerging from the horn. The calculation includes the effects of reflections from the cavity walls (which are not all at liquid nitrogen temperature), losses in the horn, the antenna pattern of the horn, and the variation of the boiling point of liquid nitrogen with the barometric pressure in the laboratory (which is measured). The noise temperature at the output reference plane is typically about 80 K. The second noise-temperature standard used in the system is the ambient standard. This consists of a commercial WR-28 termination with a small hole drilled in the side. A thermistor is inserted through the hole and into the load inside the waveguide, to monitor its temperature. The termination is then encased in a water jacket. Water from a constant-temperature bath is circulated through the water jacket to keep the termination at a constant temperature. The temperature of the ambient standard is kept within a few tenths of a kelvin of 296 K; the value used in all computations is the thermistor reading.

The water from the constant-temperature bath is also used to control other parts of the system whose temperature might otherwise differ significantly from the ambient temperature. The temperature control is important because the correction for noise power added by lossy components, eq (1), is dependent on the temperature. The derivation of our radiometer equation, eq (5), assumed that all lossy components between planes 3 and 0 and between 2 and 0 were at ambient temperature, the same as the ambient standard. This is accomplished by encasing all relevant components in water jackets. The water first flows to the ambient standard, where a thermistor measures the temperature. It then circulates through the jackets on the other components of the system and back to the water bath. A parallel water circuit is used to maintain the standard horn of the cryogenic standard at ambient temperature. The

temperature of the water is measured as it emerges from the horn, and we require that it be within 0.6 K of the ambient temperature. In addition, the temperature of the laboratory is maintained at 23 ± 0.5 °C, and it is continuously monitored and recorded. In general, the noise-temperature measurements are insensitive to small deviations from ambient in the temperature of lossy components; these are small corrections to small corrections. The measurements are, of course, sensitive to small variations in the temperature of the ambient standard, which is why its temperature is monitored by the thermistor. The relative humidity of the laboratory is also monitored and controlled; it is maintained at 40 percent ± 5 percent.

A photograph of the radiometer system, without the cryogenic standard or DUT attached, is shown in figure 3. The input switch S1 is at the far right side. The horizontal section to the left of the switch is the directional coupler. The vertical arm emerging from the coupler contains the isolator, I3 in figure 2(b). The horizontal arm from the coupler is the noise measurement path, which proceeds through the two isolators I1 and I2, which are encased in the tubular water jacket in the photograph. A short waveguide section containing the low-pass filter LPF1 leads from the isolators to the switch S3, which is located near the middle of the photograph. Just above S3 is the mixer, with the IF emerging from the front, out of the page. The IF output goes down and to the right into the variable attenuator A2 and the IF amplifier, with the amplifier output concealed behind it, going into the page and to the electronics rack. To the left of the switch S3 is a large rectangular water jacket containing the "bare" six port and its power sensors. The local oscillator is at the far left end of the radiometer, with power supplied through the dark cable and temperature-control water through the two clear tubes. To the right of the oscillator are the isolator I4, the attenuator A1, and a coupler, followed by the switch S2. The upper switch port feeds into the mixer, and the port on the right side feeds into the six port. The rectangular box in the left foreground is the power supply for the local oscillator. A few noise sources and impedance standards also lie on the bench top.
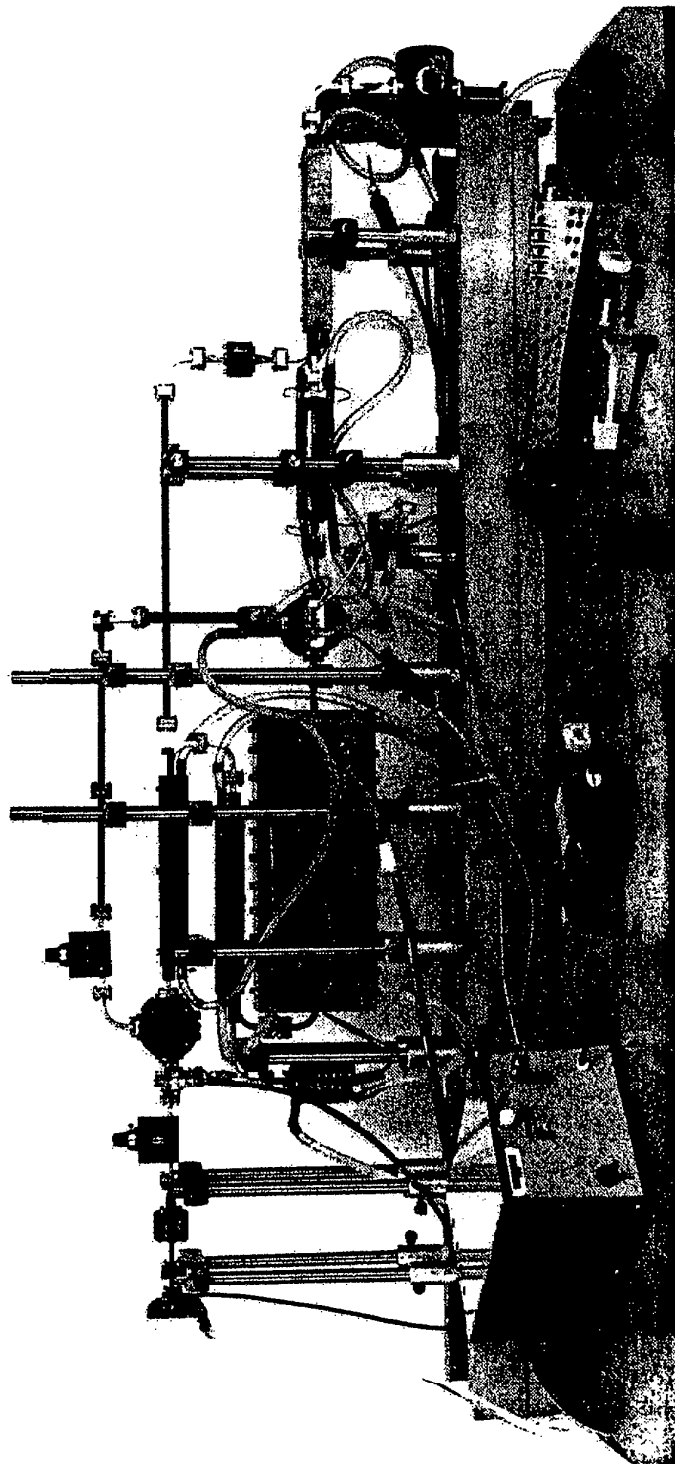
Figure 3. Photograph of WR-28 system.

11

3. MEASUREMENT PROCEDURES

A noise-temperature measurement on one of our waveguide radiometers begins with a system calibration and check, comprising an IF linearity check, calibration of the system six-port, and measurement of the asymmetry between the measurement path beginning at the DUT port and the path beginning at the cryogenic standard port. The IF linearity test consists of a series of measurements of the detected power p_x of a hot noise source for a variety of settings of the IF attenuators A3 and A4. The ratio of the power measured with a given attenuator setting to the power measured with 3 dB more attenuation is plotted as a function of detected power. The system is considered to be linear as long as the ratio of powers does not deviate by more than 0.005 dB from its low-power value. In the actual measurement, all detected powers are required to be in the linear range. Typically, the linear range extends above 3 mW, and in most noise-temperature calibrations, the detected power is kept below 2 mW.

The system six port is calibrated by attaching a series of impedance or reflection standards to the two measurement ports, the DUT port and the cryogenic-standard port, ports 2 and 3 in figure 1. The standards used are a flat short, a sliding short, and a sliding load; and the method is described in references [5] and [6]. The precise locations of the reference planes at the two measurement ports are defined by the six-port calibration. The reflection coefficient of each standard is modelled at the waveguide flange of the standard. Consequently, the system six port is calibrated to the reference plane defined by the surface of the waveguide flange at each of its measurement ports. This means that the noise temperature of the standard must be known at this reference plane (it is) and that the noise temperature measured for the DUT is at this reference plane. Once the six-port is calibrated, the operator measures the reflection coefficients of the two measurement ports, the cryogenic standard, the DUT, the check standard(s) to be used in the noise-temperature measurement, and the two auxiliary standards to be used in the asymmetry measurement. The measured reflection coefficients are compared to the historical data for the devices, to confirm that the six-port has been properly calibrated, and the DUT reflection coefficient is checked to see that

it is below 0.2 in magnitude. A larger reflection coefficient would result in unacceptably large uncertainties.

The final step of the system calibration is the measurement of the asymmetry, which is the ratio of efficiencies η_{03}/η_{02} appearing in the radiometer equation, eq (5). In principle, we can determine the asymmetry from measurements with the system six port, but in practice we use a "manual" method [3], which is more accurate and robust. The basic idea is that to measure the difference between the two measurement paths, we just attach the same source to the two ports (planes 3 and 2 in figure 1), measure the two different delivered powers, and make appropriate corrections for differences in ambient contributions and mismatch factors. The detailed implementation of that basic idea is as follows. A noise source x is connected to the two measurement ports and the delivered power is measured in each case, as is the delivered power from the ambient standard at port 1. We refer to the case with the source attached to the cryogenic-standard port (reference plane 3) as x and the case with it attached to the DUT port (plane 2) as x'. From eq (2) the equations for the three measured powers are

$$
\begin{aligned}
P_x &= M_{3,x}\eta_{03}\,(P_x - P_a) + M_{0,x}P_a + p_{ex}\, , \\
P_{x'} &= M_{2,x'}\eta_{02}\,(P_x - P_a) + M_{0,x'}P_a + p_{ex'}\, , \\
P_a &= M_{0,a}P_a + p_{ea}\, ,
\end{aligned}
\tag{7}
$$

where we have used $P_{x'} = P_x$, $M_{0,x}\alpha_{03} = M_{3,x}\eta_{03}$ and $M_{0,x}\alpha_{02} = M_{2,x}\eta_{02}$. Because of the isolator, $M_{0,x} = M_{0,x'} = M_{0,a}$ and $p_{ex} = p_{ex'} = p_{ea}$, and the equations of eq (7) can be combined to yield

$$
\frac{\eta_{03}}{\eta_{02}} = \frac{Y_{x'} - 1}{Y_x - 1}\frac{M_{2,x}}{M_{3,x}}\, ,
\tag{8}
$$

where we have dropped the unnecessary prime on the mismatch subscript. Equation (8) can be used to determine the asymmetry, but it is sensitive to errors in the measurement of the mismatch factors at the two ports. We can improve the measurement significantly with relatively little additional effort by measuring two noise sources, x_1 and x_2, simultaneously, one at each port, and then interchanging them and remeasuring each [3]. We thus obtain two versions of eq (8), one for each source. We use unprimed subscripts to denote the

configuration with x_1 attached at plane 3 and x_2 at plane 2, and we use the primed subscripts to denote the configuration with the two sources interchanged. The two measurements of the asymmetry can then be combined to yield

$$\frac{\eta_{o3}}{\eta_{o2}} = \sqrt{\frac{Y_{x_1'} - 1}{Y_{x_1} - 1} \frac{Y_{x_2} - 1}{Y_{x_2'} - 1} \frac{M_{2,x_1}}{M_{3,x_1}} \frac{M_{3,x_2}}{M_{2,x_2}}} . \tag{9}$$

This is the form used for determination of the path asymmetry in the NIST waveguide radiometers. It is relatively insensitive to errors in measurement of the mismatch factors. It is also insensitive to instrument drift, which was an important concern in previous generations of radiometers.

In using eq (9) to determine the path asymmetry, four independent Y-factors are measured to determine just one quantity. The additional information contained in these redundant measurements can be used to check the consistency of the measurements and also to provide an independent measurement of the noise temperatures of the auxiliary standards used as noise sources. If we combine the measurements with a measurement of the cryogenic standard, then for each noise source we have sufficient information to determine its noise temperature and the path asymmetry. The measured noise temperatures are compared to the historical values for the noise sources to check that the system is working properly. The two independent determinations of the path asymmetry could be compared to check the consistency of the measurements which go into eq (9). In practice, the software does not compute the two determinations of the asymmetry. Instead it computes two noise temperatures for each noise source. These are then compared to each other to check the consistency of the measurements.

Once the system has been calibrated, the noise temperature of a noise source can be measured. Determination of an unknown noise temperature from eq (5) requires that we measure the mismatch factors at the DUT and cryogenic ports, the noise temperatures of the ambient and cryogenic standards, and the delivered powers from the DUT and the two standards. The measurement begins by connecting the source to be measured and the

14

cryogenic standard to their respective measurement ports and using the system's six port to measure their reflection coefficients. The reflection coefficients of the measurement ports themselves were determined in the course of the six-port calibration, and consequently the two mismatch factors can be determined from eq (6).

The noise temperature of the cryogenic standard is derived in references [7] and [8]. The boiling temperature of the liquid nitrogen in the standard is corrected for the barometric pressure in the laboratory, read from a mercury barometer. The noise temperature T_{noise} of the ambient standard is computed from the thermistor reading of its physical temperature T_{phys} using

$$k_B T_{noise} = \frac{h f}{e^{\left(\frac{hf}{k_b T_{phys}}\right)} - 1} . \tag{10}$$

This form includes quantum effects; for high temperature or low frequency it reduces to the familiar $T_{noise} \approx T_{phys}$ for passive devices. For room temperature and a frequency of 40 GHz, the difference between the two is about 0.3 percent, which is small but significant.

The delivered powers are then measured. The front-end switch is manually switched to read the powers from the two standards and the DUT, in the sequence ambient standard, cryogenic standard, ambient, DUT, ambient. The average of the two ambient readings bracketing the cryogenic or DUT reading is used in computing the Y-factor. Each power measurement consists of an average of five readings of the power meter, with each reading representing an average over 1/6 second. The detected power is monitored to be sure that it remains in the linear range of the IF subsystem. The entire sequence of five power measurements is repeated twenty times for one measurement of the DUT noise temperature. The average values are used in computing the noise temperature from eq (5), and the standard deviation of the mean for each sample is computed. The sampling times and numbers of repetitions were chosen so that the uncertainty introduced by the spread in the readings is negligible.

15

The process just outlined constitutes a single noise-temperature measurement. In measuring an unknown source, we first measure the noise temperature of a check standard and check that its reflection coefficient and noise temperature agree with past measurements. This ensures that the system has been properly calibrated and is functioning as it should. Using the same system calibration, we then perform a measurement of the noise temperature of the DUT. For a relatively new system, such as the WR-28 system, we repeat the noise-temperature measurement of the DUT three times, to verify repeatability. For a mature system, such as WR-62 or WR-42, we measure the noise temperature of the DUT just once for a given system calibration. This entire process is then repeated two more times, resulting in three independent system calibrations, each with a measurement of the DUT's and check standard's noise temperatures (three DUT measurements for each of the three calibrations in the case of a new system). The standard deviation of the mean of the three independent noise temperature measurements should be significantly less than the type-B uncertainties (Section 5). If it is not, additional measurements are made.

After the measurements have been completed, the uncertainty is evaluated, and the results are checked a final time (by someone other than the person who made the measurements) to see that they are reasonable, that the spread of measured values is small, that the system parameters (gain, system noise temperature, reflection coefficients, etc.) are consistent with past values, and that the check standard results agree with past measurements.

4. SYSTEM CHARACTERIZATION AND CHECKOUT

The NIST Noise Project has developed and formalized a series of steps to characterize and validate a new noise-temperature calibration system. The procedure is detailed in an internal document. This document defines three levels of certification for such systems. The idea is that the system must be tested and characterized at the first level before it can be used to perform special tests for customers. As the system is used in measurements over the course of months or years, additional tests of the system are performed, refinements may be made, and operators become familiar with any idiosyncracies peculiar to that system. This

16

process leads to certification at level 2, which corresponds to a mature, stable system with a significant history. Level 3 tests comprise those additional tests necessary to qualify the system for formal certification as a NIST *Calibration* Service, as opposed to a *Special Test Service* [9]. The WR-28 system has been tested and characterized at level 1, as is appropriate for a new system. In this section we review the checkout procedure and report the results of the various tests.

In principle, verification of the radiometer performance is simple. There are just a few critical features of the system required for its proper performance. The system must respond linearly to delivered power, as assumed in the derivation of the radiometer equation; it must respond only to the intended frequencies; it must correctly measure mismatch factors and efficiencies, to relate delivered power to available power; it must have good isolation, to justify our form for the radiometer equation; the software used to control the system and compute the results must be correct; and the standards used to calibrate the system must be valid. If we verify that the system meets these requirements, we can be confident that it correctly measures the noise temperature of a noise source. The checkout procedure addresses each of these critical elements individually. It also includes checks of the system as a whole. Measurements are made at the band edges and compared to measurements on other systems covering adjacent frequency bands. Measurements are also made on check standards, to establish a baseline for their history and to demonstrate that the system can actually measure practical noise sources. Besides the critical elements just mentioned, there are several characteristics of the system which are useful to know for diagnostic, predictive, or general documentation purposes. These properties include the *intrinsic noise figure or effective noise temperature* of the system itself, the pre-detector bandwidth, the post-detector integration time, the operating power of the LO, the dynamic range of the system, the calibration of the thermistors used to measure the ambient-standard and water-bath temperatures, and a schematic diagram (and photograph) of the system. The checkout procedure includes steps to measure or estimate these properties, as well as to verify the critical elements.

17

We consider the characterization steps first. Once the construction of the system is complete, a schematic diagram of the radiometer, in its final form, is required. This is similar to figure 2(b), except that it includes model and serial numbers of the components, and more detail is given of the IF section and power meter. The intrinsic noise figure, or effective input temperature, of the system controls its sensitivity. The effective input temperature T_e of the system was measured at three frequencies, at the bottom, middle, and top of the band. This was done in conjunction with the measurement of check standards discussed below. The values measured for the WR-28 system were 2396 K at 26.5 GHz, 2357 K at 33.0 GHz, and 2318 K at 40.0 GHz. The pre-detector bandwidth and the post-detector integration time are estimated using the manufacturers' specifications for the relevant components. The pre-detector bandwidth was specified to be 10 MHz to 100 MHz, but measurements indicated that it extends down to about 1 MHz. The post-detector integration time was 0.5 s. The output powers of the Gunn diodes used as the LO ranged from 50 to 290 mW, but the attenuator A1 is adjusted so that the power reaching the mixer is 20 mW. Identification and calibration data for the thermistors used in the system were entered into the system records.

The next step is to estimate the dynamic range. To avoid saturation in the radiometer's operation, the maximum allowable input noise power is estimated. The specification is that the power at every amplifier stage be 20 dB below the 1 dB compression point for that amplifier. This ensures a linearity error for the amplifier of less than 0.1 percent [10]. For this calculation, the manufacturers' specifications are used, and the power at the detector is assumed to be 1 mW. The maximum allowable DUT noise temperatures were calculated for three settings of the attenuators A3 and A4 in figure 2(b), corresponding to no attenuation, the default attenuation (7 dB for each), and maximum attenuation (11 dB for each). The resulting maximum temperatures were 43 050 K, 227 000 K, and 575 000 K. Since typical commercial noise sources seldom exceed 12 000 K in noise temperature, this represents more than adequate dynamic range.

Consideration of the critical elements begins with the software, since it is used in virtually all the other tests. The same software is used for the WR-28 system as for the

existing WR-62 and WR-42 systems. It has already been thoroughly checked and has performed successfully for several years. Nevertheless, an additional test is performed on the six-port software. The reflection coefficient of a device is measured with the six port, and the readings of the power meters are recorded. These values for the powers are read into an independent six-port simulation program, written for this purpose by a person not involved in writing the system software. The differences between the results of the two programs must be less than 10^{-9}, and they were.

Derivation of the radiometer equation, eq (5), assumed an isolated radiometer, with departures from perfect isolation treated as an uncertainty, eq (4). To keep this uncertainty at an acceptable level, the isolation should be at least 40 dB, and preferably 50 dB. To check this, the isolation provided by the two isolators I1 and I2 was measured on a vector network analyzer. The isolation exceeded 50 dB across the entire WR-28 band. The uncertainty associated with imperfect isolation is then negligible.

The harmonic response test addresses the question whether the system responds only to the frequency of interest. Because noise sources are broadband sources, there will always be higher frequencies present at the system input, and we must check that harmonics of the measurement frequency are not down converted and combined with the signal of interest. This test is usually performed by measuring the detected power from a broadband source and then repeating the measurement with a low-pass filter between the source and the measurement system. Since the WR-28 system includes a low-pass filter in its input section (LPF1 in figure 2(b)), this test was replaced by a measurement of that filter. Its insertion loss was about 58 dB above 50 GHz, compared with about 0.2 dB across the WR-28 band.

Three tests are performed to verify the linear response of the system. The IF-linearity test measures the detected power for which the IF unit becomes nonlinear. It also serves as a check that the software and hardware of the IF unit are functioning properly. This test was described above, in Section 3, since it is repeated in every calibration. The IF unit was found to be linear up to a detected power of 7.0 mW. In actual noise-temperature calibrations, the

19

detected power is kept below 2 mW. The second linearity test is the radio-frequency (RF) linearity test. The system is first calibrated and used to measure the noise temperature of a typical noise source. A 3 dB attenuator is then attached to the DUT port, and the system is recalibrated, treating the attenuator as part of the measurement system. The noise source is then remeasured with the attenuator in place, and the two measured noise temperatures must (and did) agree to within 0.5 percent. The third linearity test is the mixer linearity test, which ensures that small changes in the LO power have no significant effect on the system performance. This is done by first calibrating the system at the normal LO power and measuring a noise source. The LO power is then reduced by 3 dB, and the noise temperature of the source is remeasured. The results of the two measurements must agree to within twice the standard deviation of the mean of the readings for the measurement done with normal power. (As explained below, multiple readings are taken and averaged for each measurement.)

The mismatch factors appearing in the radiometer equation are computed from reflection coefficients measured with the system's six-port reflectometer. The verification of the six port begins during the final construction of the system, when the phase of the six port is checked. This is done before the water jacket is sealed, in case any modifications of the wiring are required. The check consists of attaching a sliding short to the DUT port and requiring that the measured phase increase as the short is pulled out, in accord with convention. The overall performance of the system six port is checked by comparing measurements made with it to results of the same measurements made with either a vector network analyzer or the six port maintained by the Network Analysis and Measurements Project of the NIST Microwave Metrology Group. The first measurements were made on the radiometer itself, looking into the DUT port, plane 2 in figure 1 or 2(a). The real and imaginary parts of the reflection coefficient were measured at 26.5 GHz, 33.0 GHz, and 40.0 GHz using both the system six port and the network analyzer. The two measurements were required to agree within 0.014, which corresponds to the worst-case uncertainty (approximately 3σ) for the network analyzer measurements in the WR-28 band, and they did so. We shall use ± 0.007 as the standard uncertainty (1σ) in the measurements of real and

imaginary parts of reflection coefficients measured with the system six port. Additional measurements were made on four different artifacts attached to the DUT port. The artifacts comprised a 3 dB attenuator terminated with a flush short, a 3 dB attenuator terminated with an offset short, a solid-state noise source (turned on), and a matched load. Again, measurements were made at 26.5 GHz, 33.0 GHz, and 40.0 GHz on each artifact, and agreement between the system six port and the network analyzer was within 0.014 for both real and imaginary parts, for each device at each frequency.

In measuring the noise temperature of an unknown device, the system six port is used to measure the reflection coefficients needed to determine the mismatch factors, using eq (6). The six port could also be used to determine the asymmetry, which is the ratio of efficiencies η_{o2}/η_{o2} appearing in the radiometer equation, eq (5). As discussed above, however, we can measure the asymmetry more reliably using the "manual" method described in Section 3 than we can with the six port, and so we use the manual method in our measurements. The manual asymmetry method contains a check which is applied each time the method is used. In measuring the asymmetry, the delivered powers from the two auxiliary standards are measured both on the DUT port and on the cryogenic-standard port. The software automatically records the powers, Y-factors, and reflection coefficients from these measurements. Then, when the cryogenic standard is measured on its port, we have sufficient information to compute the noise temperature of each auxiliary standard two different ways. One way uses the Y-factor measured when the auxiliary standard was connected to the DUT port, treating the auxiliary standard as a DUT and using eq (5) with the measured asymmetry. The other way uses the Y-factor measured when the auxiliary standard was attached to the cryogenic-standard port. In this second case the noise temperature can be computed *without using the asymmetry*, since the noise source being measured is attached to the same port as the cryogenic standard. For each auxiliary standard we then have two noise- temperature measurements, one which used the asymmetry and one which did not. We require that the two results agree with each other and also with past measurements on that auxiliary standard.

21

The final test of a new system is a measurement of one or more known noise sources, or a comparison to existing systems in adjacent bands. This checks the proper performance of the system as a whole. For this test we measured the noise temperature at 26.5 GHz of our WR-42 primary standard, using a WR-42 to WR-28 taper. The effect of the taper was accounted for by the method developed in references [11] and [12]. The measured value of the noise temperature was 76.71 K, whereas the value calculated by the program for the standard was 76.66 K. The difference is 0.05 K or 0.07 percent, which is far smaller than the uncertainties in either the standard's temperature or the measurement procedure. Once all the tests were completed, the noise temperatures of two solid state noise sources were measured several times to begin their recorded histories. They will then be remeasured in conjunction with all future calibrations to ensure that the system has not changed significantly.

5. UNCERTAINTIES

The uncertainty analysis for the current generation of NIST total-power noise radiometers, both coaxial and waveguide, will be presented elsewhere [13]. Here we review the results for the WR-28 system. The equation used to compute the noise temperature of the DUT is eq (5), where a perfect isolator is assumed, as is a linear radiometer. Uncertainties in T_x arise due to uncertainties in the determination of the quantities appearing on the right side of eq (5) and due to departures from perfect isolation and linearity. In keeping with the notation of references [14] and [15], we use u_{Tx} to denote the standard uncertainty in the measurement of T_x. We deal first with type-B uncertainties; the type-A uncertainty and the statistics of combining multiple measurements will be treated near the end of this subsection. We use $\mathscr{E}_z$ to denote the fractional standard uncertainty in the parameter z. Thus, for example, $\mathscr{E}_{Cry} = u_{TCry}/T_{Cry}$.

The uncertainty in the noise temperature of the cryogenic standard contributes to the uncertainty in T_x as

$$\frac{u_{T_x}(Cry)}{T_x} = \left|1 - \frac{T_a}{T_x}\right| \left|\frac{T_S}{T_a - T_S}\right| \mathscr{E}_{Cry} .$$ (11)

22

The fractional uncertainty in the WR-28 cryogenic primary standard is $\mathscr{E}_{Cry}$ = 0.17 percent [13]. This is the most accurate of the NIST waveguide primary standards, due to the fact that the horn antenna and associated waveguide are fabricated of solid copper, and consequently the standard does not suffer from uncertainties associated with characterization of the behavior of a plated conductor. For a typical, high-temperature DUT, with noise temperature of 10,000 K, this results in an uncertainty in T_x of approximately 0.06 percent, or about 0.12 percent for an expanded (2σ) uncertainty. This will prove to be a minor contribution to the combined uncertainty. The other primary noise standard used is an ambient-temperature load. Its temperature is measured directly by a calibrated thermistor. The uncertainty in the temperature of the ambient standard is 0.1 K, corresponding to $\mathscr{E}_{T_a}$ = 0.034 percent. This results in a contribution to the uncertainty in the DUT noise temperature of

$$\frac{u_{T_x}(amb)}{T_x} = \left|\frac{T_x - T_a}{T_a - T_s}\right| \frac{T_a}{T_x} \times 0.034\% . \tag{12}$$

For a typical high-temperature source this results in an uncertainty of about 0.05 percent in T_x.

The power ratios Y_s and Y_x are determined from measurements of the delivered powers, using a NIST Type-IV power meter [4]. The uncertainty in the term involving the power ratios has been analyzed in references [16] and [13]. If we let $Y = (Y_x-1)/(1-Y_s)$, the result for the contribution to the fractional uncertainty in T_x is

$$\frac{u_{T_x}(Y)}{T_x} \leq \left|1 - \frac{T_a}{T_x}\right| \times 0.04\% , \tag{13}$$

which typically is negligible.

The ratio of mismatch factors in eq (5) is one of the principal sources of uncertainty. The standard uncertainty in the ratio of mismatch factors will be denoted u_{MM}. It depends on the correlation between variations in the measurements of different reflection coefficients, which are measured with the system's six-port reflectometer. If such variations are all perfectly correlated,

23

$$u_{M/M}(cor.) = 4 \, u_{\mathrm{Im}\Gamma} \, |y_s + y_{3,R} - y_x - y_{2,R}| \, , \tag{14}$$

where x and y refer to real and imaginary parts of Γ, and where we have assumed that the reflection coefficients are small. This is the corrected version of the form in reference [3]. If, on the other hand, the variations are all completely uncorrelated,

$$u_{M/M}(uncor.) = 2\sqrt{2} \, u_{\mathrm{Re}\Gamma} \, [\, (x_s - x_{3,R})^2 + (y_s + y_{3,R})^2$$
$$+ (x_x - x_{2,R})^2 + (y_x + y_{2,R})^2]^{\frac{1}{2}} \, , \tag{15}$$

where we have used $u_{\mathrm{Re}\Gamma} = u_{\mathrm{Im}\Gamma}$. For WR-28 the uncertainty in our measurements of real or imaginary parts of reflection coefficients is [13] $u_{\mathrm{Re}\Gamma} = u_{\mathrm{Im}\Gamma} = 0.007$. Since we do not know the degree of correlation between uncertainties in the measurements of the different reflection coefficients, we will use the greater of eqs (14) and (15),

$$u_{M/M} = Max\{u_{M/M}(cor) \, , \, u_{M/M}(uncor)\} \, . \tag{16}$$

The resulting uncertainty in the DUT noise temperature is then

$$\frac{u_{T_x}(M/M)}{T_x} = \left| 1 - \frac{T_a}{T_x} \right| \times Max\{u_{M/M}(cor) \, , \, u_{M/M}(uncor)\} \, , \tag{17}$$

where we have used the fact that the ratio of mismatch factors is very near 1, and therefore $\mathcal{E}_{MM} = u_{MM}/(M/M) \approx u_{MM}$. Equation (17) leads to typical uncertainty contributions of about 0.3 percent to 0.5 percent for WR-28, for sources with reflection coefficients less than 0.1.

The measurement of the path asymmetry η_{03}/η_{02} was discussed in Section 3. The asymmetry is given by eq (9),

$$\frac{\eta_{03}}{\eta_{02}} = \sqrt{\frac{Y_{x_1'} - 1}{Y_{x_1} - 1} \frac{Y_{x_2} - 1}{Y_{x_2'} - 1} \frac{M_{2,x_1}}{M_{3,x_1}} \frac{M_{3,x_2}}{M_{2,x_2}}} \, , \tag{18}$$

where the Y factors are the ratios of the delivered power from the designated source to the delivered power from the ambient standard, $Y_{x_1}' = p_{x_1}'/p_a$, etc. The uncertainty in this

determination of the asymmetry is dominated by the uncertainty in the measurement of the ratios of mismatch factors. Using typical values of reflection coefficients, the uncertainty in the asymmetry is $u_{\eta/\eta} \approx 0.4 \times u_{R_{s}\Gamma} = 0.28$ percent for WR-28. The resulting uncertainty in the DUT noise temperature is

$$\frac{u_{T_x}(\eta/\eta)}{T_x} = \left| 1 - \frac{T_s}{T_x} \right| \times 0.28\% , \qquad (19)$$

which is one of the largest components of the uncertainty. There is also an uncertainty that arises from the variability from one waveguide flange to another, even when both meet the specifications. Such variations are already included in our estimates of $u_{R_{s}\Gamma}$, and they require no further special treatment for their effects on mismatch factors. They do, however, affect the measurement of the asymmetry, and this effect was not included in $u_{Ix}(\eta/\eta)$. When the asymmetry is measured, diode noise sources are attached to the ports of interest, and the delivered powers are measured. When this asymmetry is used in a calibration, we assume that the connectors of the DUT and the primary standard are identical. The error in that assumption can be written as

$$\frac{\Delta T_x}{T_x} = \left| 1 - \frac{T_s}{T_x} \right| \left| \frac{\eta_{sc}}{\eta_{xc}} - 1 \right| , \qquad (20)$$

where the last term contains the ratio of the efficiencies of the cryogenic-standard connector and the DUT connector. This last term was estimated in reference [3]. Subsequent revisions resulted in an approximate value of ± 0.003 dB $\times f^{1/2}$(GHz) for the range of $|\eta/\eta\text{-}1|$, which we will use as the standard uncertainty in that quantity. To convert from decibels to a natural number we multiply by 0.23, thereby obtaining

$$\frac{u_{T_x}(conn)}{T_x} = 0.069\% \left| 1 - \frac{T_s}{T_x} \right| \sqrt{f} , \qquad (21)$$

where f is in gigahertz. This is a sizable contribution to the uncertainty, roughly 0.4 percent for a typical device at 36 GHz, and is probably an overestimate. An improved analysis could reduce this uncertainty significantly.

25

The form for the worst-case error due to neglecting $(\Delta T_x)_{i_2}$ in eq (4) was derived in reference [3] for 50 dB isolation. The isolation at the front end of the radiometer was measured to be greater than 50 dB across the entire WR-28 frequency band. Converting that worst-case error to a standard uncertainty and correcting a minor arithmetic error in reference [3] results in [13]

$$\frac{u_{T_x}(isol)}{T_x} = \left\{ 0.24 \, |\Gamma_S| \left| 1 - \frac{T_a}{T_x} \right| + 0.024 \left| 1 - \frac{T_S}{T_x} \right| + 54 \, \frac{|\Gamma_x|}{T_x} \right\} \, \% \, . \tag{22}$$

For a typical DUT this uncertainty is about 0.05 percent, which is negligible.

The six-port reflectometer of the system measures reflection coefficients at what is, for present purposes, a single frequency, the nominal calibration frequency. The noise power, however, is measured over a finite IF bandwidth, and the range of RF frequencies contributing to this measurement band could be offset from the nominal calibration frequency by the IF frequency. The uncertainty introduced by the possible variation of the reflection coefficients across the measurement band is called the broadband mismatch uncertainty, and the uncertainty due to the offset between the frequency of the noise power measurement and the calibration frequency is called the frequency offset uncertainty. Both effects were calculated in references [3] and [17], with slightly different results. The form we use [13] is based on [3],

$$\frac{u_{T_x}(BBMM)}{T_x} = \frac{200\%}{\sqrt{3}} \left| \cos\left(\frac{4 \, \pi \, f_{IF} \, l_e}{30}\right) sinc\left(\frac{\pi \, B \, l_e}{15}\right) - 1 \right|$$

$$\times \, (|\Gamma_S \Gamma_{3,R}| + |\Gamma_x \Gamma_{2,R}|) \left| 1 - \frac{T_a}{T_x} \right| \, . \tag{23}$$

with

$$l_e = l \sqrt{1 - \frac{f_c^2}{f^2}} \, . \tag{24}$$

For the WR-28 system, the parameter values are $f_{IF} = 0$, $l = 50$, $B = 0.04$, and $f_c = 21.1$ GHz. Because $f_{IF} = 0$, the frequency offset error vanishes, and we are left only with the effect of the broadband mismatch. This contribution to the total uncertainty is typically negligible.

The final contribution to the type-B uncertainty is due to the possibility of small nonlinear behavior by the radiometer. The radiometer is tested for linearity in the initial checkout procedure, and an additional routine linearity check is performed before each measurement of a customer's device. This routine linearity check can be used to place a limit on the uncertainty due to nonlinear behavior. The test consists of switching a (nominally) 3 dB attenuator in and out of the circuit in front of the IF amplifier. The ratio of the two output powers is measured and plotted as a function of input power. The "linear" result is established by averaging the low-power points, and we then require that the measured ratio not deviate from the "linear" result by more than 0.005 dB (0.12 percent). This allows us to deduce [13]

$$
\frac{u_{T_x}(lin)}{T_x} = \left| 1 - \frac{T_a}{T_x} \right| \frac{u_{Y_x}}{|Y_x - 1|}
$$

$$
= \frac{u_{Y_x}}{Y_x} = 0.06\%
$$

(25)

for the uncertainty in T_x due to departures from linearity.

The type-B standard uncertainty for a single noise temperature measurement is obtained by forming the square root of the sum of the squares of the individual contributions eqs (11, 12, 13, 17, 19, 21, 22, 23, 25),

$$
u_B = [u_{T_x}^2(Cry) + u_{T_x}^2(amb) + u_{T_x}^2(Y) + u_{T_x}^2(M/M) + u_{T_x}^2(\eta/\eta)
$$
$$
+ u_{T_x}^2(isol) + u_{T_x}^2(con) + u_{T_x}^2(BBMM) + u_{T_x}^2(lin)]^{1/2} .
$$

(26)

In measuring a customer's device, we make several measurements of the DUT noise temperature. Because the uncertainty defined by eq (26) depends on the measured noise temperature and on various measured reflection coefficients, it is in principle different for each of the separate measurements of the DUT noise temperature. In practice, however, there

27

is little difference between the values, and we use the maximum.

To evaluate the type-A uncertainty, we consider those measurements which are repeated several times and which thus present the opportunity for a statistical evaluation of their uncertainty. As described in Section 3, we perform multiple measurements of each delivered power (p_a, p_j, p_x) for a single measurement of the noise temperature, and we perform several independent measurements of the noise temperature to obtain the final result. For each quantity, we take the type-A uncertainty to be the standard deviation of the arithmetic mean of the measurements. For the power measurements, the number of measurements and the sampling time were chosen large enough that the type-A uncertainty is negligible in each case. The sole significant type-A uncertainty arises from the repetition of the entire noise-temperature measurement. For the mature systems (WR-62, WR-42), we perform three or more independent measurements of T_x, performing an independent system calibration for each. The type-A uncertainty for these cases is the standard deviation of the mean of the set of values measured for T_x. The situation is somewhat more complicated for a new system, such as WR-28. For such systems, three or more independent system calibrations are performed, but several noise temperature measurements are made for each calibration. The spread among the measurements for each calibration is small compared to the variations from calibration to calibration, however, and so again we just use the standard deviation of the mean of the set of average noise temperatures. If we let $<T_x>_i$ be the average of the noise temperature measurements for a given system calibration (i), then the final result for the measured noise temperature is

$$T_x = \frac{1}{N} \sum_1^N <T_x>_i \, ,$$

(27)

and the type-A uncertainty is

$$u_A = \sqrt{\frac{1}{N(N-1)} \sum_1^N (<T_x>_i - T_x)^2} \, .$$

(28)

For typical measurements with the waveguide radiometers, u_A is less than about 0.2 percent. The expanded ($k = 2$) combined uncertainty is computed from eqs (26) and (28),

28

$$U = 2\sqrt{u_A^2 + u_B^2} \, . \tag{29}$$

The uncertainty was computed for the initial measurements of the check standards, to obtain an indication of the uncertainties we can expect in calibrations of WR-28 noise sources. The expanded combined uncertainty varied with source and frequency, but the values fell between 1.2 percent and 1.5 percent.

6. SUMMARY

The NIST Noise Project has recently completed constructing and testing a noise-temperature measurement system for noise sources with WR-28 waveguide flanges. This paper presented the derivation of the radiometer equation for the system, a description of the system, an outline of the procedures for a noise-temperature measurement, a detailed review of the tests used to verify that the system is functioning properly, and the uncertainty analysis. The derivation of the radiometer equation, the measurement procedures, the checkout procedure, and the general system design also apply to the other NIST waveguide systems for measuring noise temperature (WR-62 and WR-42 at present).

---

7. REFERENCES

[1]   Dicke, R.H. The measurement of thermal radiation at microwave frequencies. Rev.
       Sci. Instrum. 17(7): 268-275; 1946 July.

[2]   Miller, C.K.S.; Daywitt, W.C. The NBS switching radiometers. Nat. Bur. Stand.
       (U.S.) Internal Report 84-3004; 1984 May.

[3]   Daywitt, W.C. Radiometer equation and analysis of systematic errors for the NIST
       automated radiometers. Natl. Inst. Stand. Technol. Tech. Note 1327; 1989 March.

[4]   Larsen, N.T. A new self-balancing DC-substitution RF power meter. IEEE Trans.
       Instrum. Meas. IM-25(4): 343-347; 1976, December.

[5]   Engen, G.F. Calibration of an arbitrary six-port junction for measurement of active
       and passive circuit parameters. IEEE Trans. Instrum. Meas. IM-22(4): 295-299; 1973
       December.

[6]   Hoer, C.A. Using six-port and eight-port junctions to measure active and passive
       circuit parameters. Nat. Bur. Stand. (U.S.) Tech. Note 673; 1975 September.

[7]   Daywitt, W.C. Design and error analysis for the WR10 thermal noise standard. Nat.
       Bur. Stand. (U.S.) Tech. Note 1071; 1983 December.

[8]   Daywitt, W.C. The noise temperature of an arbitrarily shaped microwave cavity with
       application to a set of millimeter wave primary standards. Metrologia 30: 471-478;
       1993/1994.

[9]   Simmons, J.D. NIST calibration services users guide 1991. Natl. Inst. Stand.
       Technol. Special Publication 250, Ch. 1C; 1991 October.

[10]   Cohn, C.E. Errors in noise measurements due to finite amplitude range of the measuring instrument. Rev. Sci. Instrum. 35: 701-703; 1964 June.

[11]   Daywitt, W.C. Determining adapter efficiency by envelope averaging swept frequency reflection data. IEEE Trans. Microwave Theory Tech. MTT-38(11): 1748-1752; 1990 November.

[12]   Pucic, S.P.; Daywitt, W.C. Single-port technique for adapter efficiency evaluation. 45th ARFTG Conference Digest; Orlando, FL; 1995. 113-118.

[13]   Randa, J. Uncertainties in NIST noise-temperature calibrations at and above 1 GHz. Natl. Inst. Stand. Technol. Internal Report; in preparation; 1997.

[14]   ISO Guide to the Expression of Uncertainty in Measurement. International Organization for Standardization; Geneva, Switzerland; 1993.

[15]   Taylor, B.N.; Kuyatt, C.E. Guidelines for evaluating and expressing the uncertainty of NIST measurement results. Natl. Inst. Stand. Technol. Tech. Note 1297, 1994 edition; 1994 September.

[16]   Pucic, S.P. The uncertainty in Y-factor measurements. URSI National Radio Science Meeting Digest; Boulder, CO; 1995. 39.

[17]   Perera, S. Broadband mismatch error in noise measurement systems. Conference on Precision Electromagnetic Measurements Digest; Paris; 1992. 256-257.